Transmit and receive FDTD modeling as a valuable tool for RF coil development: validation of simulations with in vivo torso imaging at 7 Tesla

C. Akgun[1], C. J. Snyder[1], S. Moeller[1], P. J. Bolan[1], T. Vaughan[1], K. Ugurbil[1,2], P-F. Van de Moortele[1], and G. Metzger[1]

[1]CMRR/Radiology, University of Minnesota, Minneapolis, MN, United States, [2]Hochfeld-Magnetresonanz-Zentrum, Max Planck Institut fur Biologische Kybernetik

Introduction:

The ability to predict both transmit and receive characteristics in vivo is an important and necessary tool for the development of coils especially at ultra high magnetic fields (UHF). Accurate simulation permits the virtual development of coils saving both human and material resources [1, 2]. This is especially important during this period where large arrays and complex geometries are being proposed to maximize parallel imaging performance [3-5], B1+ shimming flexibility [6,7] and receive sensitivity [8] while simultaneously managing local RF deposition. Finite difference time domain (FDTD) simulations can provide a wealth of information including element specific B1 and electric fields (E-fields) to determine geometry factors, evaluate B1+ shimming performance and to calculate subsequent SAR distributions. In this paper we present several examples of where simulated results compare well with experimental data in torso imaging at 7 Tesla with a focus on the prostate. Confidence in these simulations will prospectively guide the development of future RF coils and optimization strategies.

Methods: *Experimental*

Two flexible TEM transceiver arrays were built; 8 and 16 channel. The physical geometry of the individual coil elements were 15.3 cm in length with a 5.0 cm ground conductor and a 1.27 cm inner conductor and a 1.27 cm thick PTFE dielectric. The elements for a given coil were evenly distributed between two identical PTFE plates which were placed anteriorly and posteriorly on the body at the level of the prostate. The distance between element centers on a given plate were 4.3 cm and 2.1 cm for the 8 and 16 channel arrays, respectively. Each channel was tuned to the proton Larmor frequency at 7T and capacitively decoupled from the nearest neighbor element. All imaging experiments were performed using a Siemens console and whole body gradients. B1+ shimming was employed to optimize the transmit phase for each element in the array [7].

Methods: *Modeling*

Numerical Maxwell solutions of the 8 and 16 channel stripline transceiver arrays were calculated with an anatomically correct human body model using XFDTD (Remcom Inc., State College, PA). The body and coil array were modeled at a resolution of 5 mm with coil dimensions presented in the experimental section. Each channel was driven by one current source and tuned to the Larmor frequency at 7T for the prostate region in the model. Each channel was simulated individually and later combined with their geometric phases and/or B1+ shim phases. The net input power for each coil was used to normalize each respective coil element.

Parallel imaging performance was evaluated at a central axial slice by providing mean and maximum geometry factors (g-factors) for combined reduction factors up to 8 and 16 for the 8-channel and 16-channel arrays respectively. The "mean" values given are the average g-factors from the center slice of the 3D acquisition while the "max" values represent the worst case within the slice as this is a spatially varying parameter. Theoretical values were calculated from the Remcom software output while the experimental results were determined from in vivo data acquired with a gradient echo sequence similar to that used for dynamic contrast enhanced imaging (T1 weighted 3D GRE, resolution 1.6 x1.6 x 4 mm).

	Experimental				Remcom			
8-channel	A-P, R=1		A-P, R=2		A-P, R=1		A-P, R=2	
	Mean	Max	Mean	Max	Mean	Max	Mean	Max
L-R, R=1	1	1	1.04	1.28	1	1	1.01	1.14
L-R, R=2	1.03	1.17	1.08	1.45	1.03	1.18	1.04	1.27
L-R, R=3	1.15	1.62	1.28	1.99	1.13	1.60	1.17	1.72
L-R, R=4	1.30	2.03	1.59	2.97	1.27	1.89	1.38	2.58

Fig 1. Parallel imaging performance: experimental versus theoretical (8 channel array)

	Experimental				Remcom			
16-channel	A-P, R=1		A-P, R=2		A-P, R=1		A-P, R=2	
	Mean	Max	Mean	Max	Mean	Max	Mean	Max
L-R, R=2	1.01	1.1	1.05	1.30	1.01	1.06	1.02	1.09
L-R, R=4	1.11	1.36	1.21	1.65	1.10	1.35	1.12	1.39
L-R, R=6	1.27	1.84	1.60	2.73	1.33	1.59	1.27	2.02
L-R, R=8	1.58	2.78	3.17	+10	1.52	2.54	1.72	3.44

Fig 2. Parallel imaging performance: experimental versus theoretical (16 channel array)

Results / Discussion:

On the receive side it is very important to be able to investigate and compare achievable reduction factors with different coil geometries. Figures 1 and 2 show the extremely close correspondence at 7 Tesla between simulated and measured g-factors for the 8 and 16 channel coils, respectively, thus indicating that simulations can accurately model the complex B1- patterns present at UHF. As expected, higher accelerations were observed for the 16 channel coil both experimentally and from simulation while still maintaining reasonable performance (i.e. mean g-factors < 1.4). The realization of these high reduction factors permitted an 8-fold reduction in scan time for the 3D acquisition described above resulting in a temporal resolution of 4 s as compared to 32 s without acceleration.

On the transmit side, modeling B1+ and E-fields are important for optimizing transmit efficiency and homogeneity but, even more so, for understanding and developing methods to manage local SAR. Figure 3 shows the fractional available B1+ maps from both simulated and experimental data after B1+ shimming. The available B1+ maps are quite similar as the 'S'-shaped pattern of high transmit efficiency (red) observed in the experimental data (right) is also observed in the simulated data (left). This data gives confidence that the simulated E-fields and the SAR values calculated from them are also correct. The availability of accurate E-fields for a given subject will provide valuable information for optimization routines taking into account constraints minimizing local SAR. An example of modeling SAR is shown in Figure 4, where the ultimate affect of B1+ shimming results in the reduction in local hot spots in the periphery for a given B1+ in the prostate.

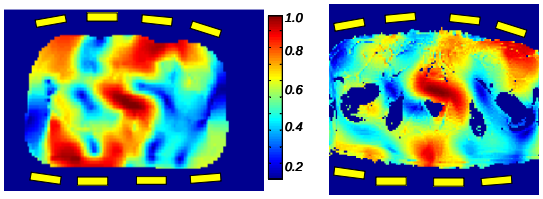

Fig 3. Fractional available B1 maps determined for the prostate from simulation (left) and experiment (right).

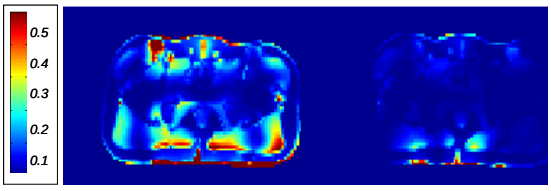

Fig 4. Theoretical SAR demonstrating local SAR before and after shimming for an equal B1+ within the prostate.

Conclusions

Agreement between our experimental results and simulation was excellent. With respect to coil receive characteristics, parallel imaging performance was accurately predicted through simulation. With respect to transmit characteristics, B1+ fields manipulated through B1 shimming methods were predicted accurately by the FDTD solver. These findings build confidence in our ability to evaluate SAR for the development of future optimization procedures.

References : [1] Ibrahim T et al. Proc. of the 14th meeting of the ISMRM 2005,820. [2] Collins CM et al. Magn. Reson. Med. 54:1327-1332, 2005. [3] Vaughan J.T. et al. Proc..of the 14th meeting of the ISMRM 2006,213. [4] Snyder, C. et al. Proc. of the 15th meeting of the ISMRM 2007,164. [5] Roemer PB. et at. Magn Reson Med 1990 ; 16: 192-225. [6] Van de Moortele et al. Intl. Symp. on Biomedical MRI and Spectroscopy at Very High Fields 2006. [7] Metzger, GJ Magn Reson Med 2007; in press [8] Wiesinger et al. Magn Reson Med 2004; 52: 953-964.

Acknowledgements: This work was funded by BTRR - P41 RR008079; NIH-R01 EB000895; NIH R01-CA0094200